

UKAEA-CCFE-PR(20)120

T. Long, J.S. Allcock, L. Nie, R. M. Sharples, M. Xu, R.
Ke, S. Zhang, S. A. Silburn, J. Howard, B. Yuan, Y.
Yu, Z.H. Wang, X.M. Song, L. Liu

Doppler Coherence Imaging Spectroscopy Diagnostic for Scrape- off -layer Impurity Plasma Flow Measurements

Enquiries about copyright and reproduction should in the first instance be addressed to the UKAEA Publications Officer, Culham Science Centre, Building K1/O/83 Abingdon, Oxfordshire, OX14 3DB, UK. The United Kingdom Atomic Energy Authority is the copyright holder.

The contents of this document and all other UKAEA Preprints, Reports and Conference Papers are available to view online free at scientific-publications.ukaea.uk/

Doppler Coherence Imaging Spectroscopy Diagnostic for Scrape-off -layer Impurity Plasma Flow Measurements

T. Long, J.S. Allcock, L. Nie, R. M. Sharples, M. Xu, R. Ke, S.
Zhang, S. A. Silburn, J. Howard, B. Yuan, Y. Yu, Z.H. Wang, X.M.
Song, L. Liu

Doppler Coherence Imaging Spectroscopy Diagnostic for Scrape-off-layer Impurity Plasma Flow Measurements on the HL-2A Tokamak

T. Long¹, J. S. Allcock^{2,3}, L. Nie^{1*}, R. M. Sharples², M. Xu¹, R. Ke¹, S.
Zhang^{1,4}, S. A. Silburn³, J. Howard⁵, B. Yuan^{1,4}, Y. Yu⁴, Z. H. Wang¹,
X. M. Song¹, L. Liu¹ and HL-2A team

¹ Southwestern Institute of Physics, Chengdu, China

² Centre for Advanced Instrumentation, Department of Physics, Durham University, United Kingdom

³ Culham Centre for Fusion Energy, Culham Science Centre, United Kingdom

⁴ University of Science and Technology of China, Hefei, China

⁵ The Australian National University, Canberra, Australia

Email of the main author: longt@swip.ac.cn

Abstract

A Doppler coherence imaging spectroscopy diagnostic has been developed on the HL-2A tokamak for scrape-off-layer impurity plasma flow measurements. Two-dimensional imaging of line-averaged C²⁺ flow in the high-field-side scrape off layer with time resolution up to 1 ms, has been achieved successfully by this system. The spatial angular resolution in horizontal direction is $\sim 0.023^\circ$ and the angular resolution in vertical direction is $\sim 0.25^\circ$, over a 34° field of view. A delicate calibration system has been utilized to calibrate the group delay and interference fringe pattern to allow the flow measurement error $\sim \pm 1$ km/s. In this paper, the details of optical instrument, calibration system and measurement results of Doppler coherence imaging diagnostic on the HL-2A tokamak are reported. The scrape-off-layer carbon ion flow dynamics are presented during an edge-localized mode crash.

Keywords: impurity plasma flow, coherence imaging, spectroscopy diagnostic, tokamak

1. Introduction

Impurities have important effects on the performance of fusion devices like ITER and DEMO. Excessive impurity levels will limit the fusion reaction via dilution and radiative cooling[1]. Impurity transport in the plasma scrape-off-layer (SOL) plays an important role in the erosion and deposition of the plasma-facing materials[2]. Impurity flow in the plasma edge and SOL, imposing the boundary conditions on the confined plasma and divertor region, is a good onset to study impurity behaviors[3] and the relevant physics. Doppler Coherence Imaging Spectroscopy (CIS)[4-6] is a novel diagnostic technique for imaging the time resolved impurity plasma flows at the plasma boundary and divertor. It has been applied successfully on various plasma devices, including a linear helicon plasma device[7], WEGA[8] and W7-X stellarator[9], DIII-D[10, 11] and MAST[12] tokamaks. A related technique has been proposed for tomographic reconstructions of imaging on ITER[13].

The measurement principles of Doppler CIS[4, 10] are based on the Doppler shifts of visible ion emission spectral lines and Fourier transform spectroscopy. Considering the monochromatic light emitted from plasma passes through a 2-beam interferometer with a time delay τ between these two beams, an interferogram with sinusoidal fringe can be observed:

$$S(\tau) = \frac{I_0}{2} \{1 + \xi_D \cos(\phi_0 + \phi_D)\}. \quad (1)$$

Here, I_0 is the intensity of light source. ξ_D denotes the contrast envelope of fringe. $\phi_0 = 2\pi\nu_0\tau_0$ represents the phase introduced from un-shifted time delay τ_0 of the interferometer. ν_0 is the optical frequency of the light in plasma rest frame.

$$\phi_D = \kappa(\tau_0)\phi_0 \left(-\vec{v}_D \cdot \frac{\hat{l}}{c}\right) \quad (2)$$

ϕ_D represents the phase caused by Doppler frequency shift due to line-of sight plasma flow, where $\kappa(\tau_0)$ represents the delay dispersion of birefringent crystal of interferometer[4]. The orientation of a positive v_D is directed from plasma to detector. \hat{l} is a unit vector in the line of sight direction from detector to plasma. Thus, the plasma flow can be obtained via the Doppler phase of the fringe:

$$\vec{v}_D \cdot \hat{l} = -\frac{c\phi_D}{\kappa(\tau)\phi_0}. \quad (3)$$

The remainder of this paper is organized as follows. In section 2, we introduce the doppler CIS diagnostic system for the HL-2A tokamak, including the optical system and the calibration system. In Section 2.1, the details of optical path and optical instrument are presented. In Section 2.2, the calibration hardware and calibration results are displayed. Section 3 reports the measuring results for carbon ion flow in an ELMY (edge-localized modes) H-mode discharge. Section 4 gives the summary and future work.

2. Doppler CIS diagnostic for the HL-2A tokamak

2.1 The optical system

HL-2A is a medium-size tokamak with a major radius of 1.65 m and a minor radius of 0.4 m [14-17]. It operates with $B_t \sim 1.0\text{-}2.0$ T. The Doppler CIS viewing port (diameter $\sim 105\text{mm}$) is ~ 200 mm above the outer mid plane. A stainless-steel shutter is installed in front of the quartz window of viewing port. This is to prevent it from coating during glow discharge cleaning and siliconization of the vacuum vessel. The CIS detector (i.e. a high-speed camera) must be more than 3 meters away from the magnetic field coils, to be free from the electromagnetic interference. Thus, an optical system was designed for doppler CIS diagnostic on the HL-2A tokamak, as shown by Figure 1. The light path is represented by the colored line beams.

A mirror ($100 \times 120\text{mm}$) in front of the viewing port is used to reflect the light emitted from plasma. Lens 1 is a zoom lens with focal length 70 mm, Lens 2 and Lens 3 are two prime lenses with long focal length 500 mm. These two reversed telephoto lenses can relay the optical path and reduce the vignetting of image effectively. Lens 4 and Lens 5 are another two reversed prime lenses with short focal length 150mm. The CIS interferometer lays in the collimated light region between Lens 4 and Lens 5. This static polarization interferometer is the key part of the CIS diagnostic. It is more robust and stable than a traditional interferometer, which mechanically moves a mirror to change the phase delay [18].

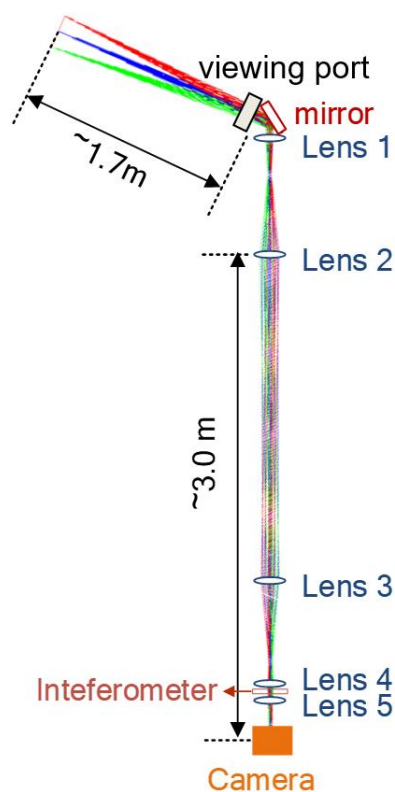


Figure 1. A schematic diagram of CIS optical system on the HL-2A tokamak.

A schematic of CIS interferometer is shown by Figure 2(a). It is composed of 4 plates of diameter ~ 2 inches. They are a polarizer, a waveplate or delay plate (thickness ~ 4.6

mm), a Savart plate (thickness ~ 4.0 mm) and an analyzer, respectively. Both delay plate and Savart plate are made from Alpha barium borate (BaB_2O_4 , α -BBO) birefringent crystal. A polarized collimated light beam is resolved to two components in the interferometer. They are an ordinary component polarized parallelly to waveplate's optic axis, and an extraordinary component polarized perpendicularly. A fixed phase delay ϕ_d is introduced by the wave plate, due to the different refractive indexes between O and E components. Then, a savart plate is used to split the O and E components spatially. It imposes an additional phase delay ϕ_s , which depends on the incident angle. The light beams are converged by Lens 5. They eventually interfere at the image plane. The angle-dependent delay sweeping leads to interferogram, as shown by Figure 2(b). The intensity can be extracted from the interferogram by filtering out the carrier fringe frequency in the Fourier domain. The instantaneous phase can then be extracted from the fringe pattern free of brightness information by a demodulation technique based on Discrete Fourier transform and Hilbert transform[19].

The precise interferometer delay is sensitive to ambient temperature of the birefringent crystal due to the thermal expansion and the thermo-optic effect. It is also sensitive to the alignment of the birefringent plates. Therefore, the interferometer is enclosed in a temperature controller to stabilize the temperature. The whole optical system is fixed on an optical table to get rid of low-frequency mechanical vibration.

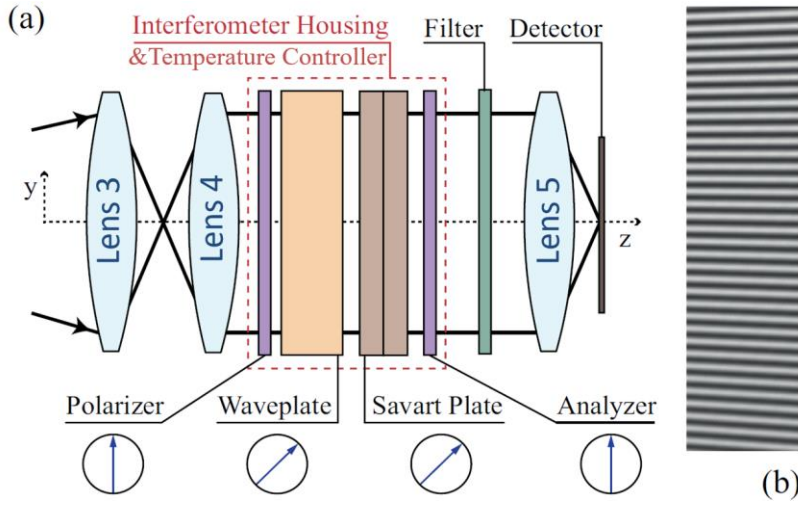


Figure 2. (a) A schematic of CIS static polarization interferometer; (b) CIS interferogram.

A custom bandpass filter in front of Lens 5 is used to isolate the targeted spectral line. Since the divertor of HL-2A tokamak is covered with carbon fiber composite (CFC) material, CIII triplet lines (464.742nm, 465.025nm, 465.147 nm) emitted from impurity ions C^{2+} are used as the targeted lines. The intensity weighted average wavelength of CIII triplet is 464.88 nm. Figure 3(a) shows the filter performance over two parameters. They are center wavelength (CWL) and full width at half maximum (FWHM) of filter's transmission profile. The filter's performance in the white region is acceptable for CIS measurement. It owns high light transmission, slight phase distortions between image core and edge, weak neighboring lines' contamination and negligible vignetting. This

calculation is based on an instrument model of reference[19] where more details can be found. In Figure 3(b), the green line shows the measured CIII triplet spectra on the HL-2A tokamak. The red dotted line indicates CIII average wavelength. The blue line shows the transmission profile of the bandpass filter.

The high-speed camera in the Figure 1 is used to shoot the interferogram. The sensor size is 35.8×22.4 mm, corresponding to an in-focus object region 927×580 mm for the CIS optical path. The frame rate capability ranges from 100 fps to 22,500 fps with full resolution 1280×800 pixels. The temporal resolution therefore is 0.05-10ms, which is only limited by light intensity. The bit depth is 12 to allow high dynamic range.

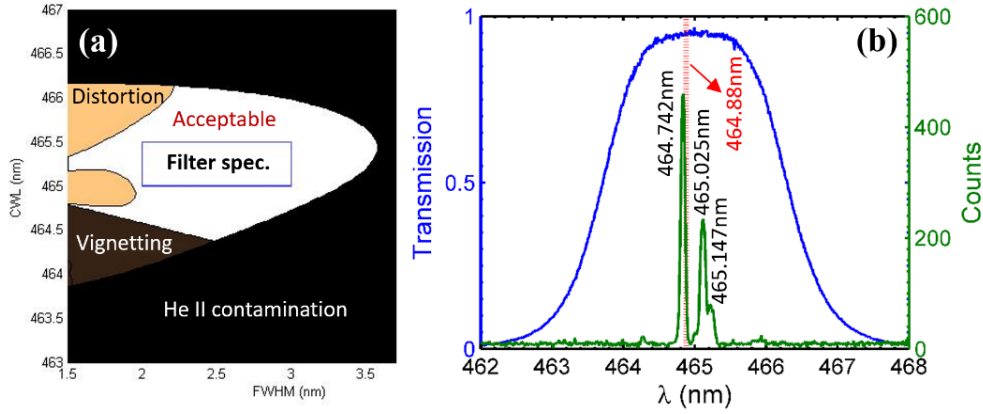


Figure 3. (a) Bandpass filter specification for CIII lines in the parameter space: CWL vs FWHM; (b) The transmission profile of the custom filter and the measured spectra on the HL-2A tokamak.

Figure 4(a) shows the field of view of Doppler CIS on the HL-2A tokamak. The viewing angle is $\sim 34^\circ$. The horizontal angular resolution is $\sim 0.023^\circ$. The vertical angular resolution depends on the scale of fringes (≈ 11 pixels per fringe for the HL-2A's CIS instrument), which then is estimated $\sim 0.25^\circ$. Figure 4(b) shows a typical equilibrium configuration reconstruction from EFIT on the HL-2A tokamak. Figure 4(c) shows a CIS raw image of plasma cross section in an H-mode discharge. The inboard vacuum chamber wall and NBI port can be seen.

2.2 The calibration system

As shown in Equation (3), the 2-D profile of plasma flow can be obtained via the phase shift of the fringe pattern relative to that produced by stationary emission. To be simplified, equation (3) could be written as equation (4). $\phi(\lambda_0)$ is the phase of fringe pattern without doppler shift. ϕ_m is the phase of fringe pattern with doppler shift when doing the measurements for tokamak plasma. $\hat{N}(\lambda_0) = \kappa(\tau_0)v_0\tau_0$ is the group delay of the birefringent crystal in the interferometer at λ_0 . Group delay is often used in interferometry as a first-order approximation for instrument dispersion[18]. To calculate the plasma flow, an accurate calibration image of the unshifted fringe pattern, i.e. fringes generated from a motionless light source, and a calibration of the group delay for target line λ_0 , are vital. With linear approximation[20, 21], the normalized phase shift is proportional to normalized wavelength shift. Equation (5) follows directly

from the definition of the group delay. $\hat{N}(\lambda_0)$ can be calibrated by fitting the slope of $\Delta\phi/2\pi$ vs $(\lambda_0 - \lambda)/\lambda$ line.

$$\phi_D = \phi_m - \phi(\lambda_0) = 2\pi\hat{N}(\lambda_0)\frac{v_D}{c} \quad (4)$$

$$\frac{\Delta\phi}{2\pi} = \frac{\phi(\lambda) - \phi(\lambda_0)}{2\pi} = \hat{N}(\lambda_0)\frac{\lambda_0 - \lambda}{\lambda} \quad (5)$$

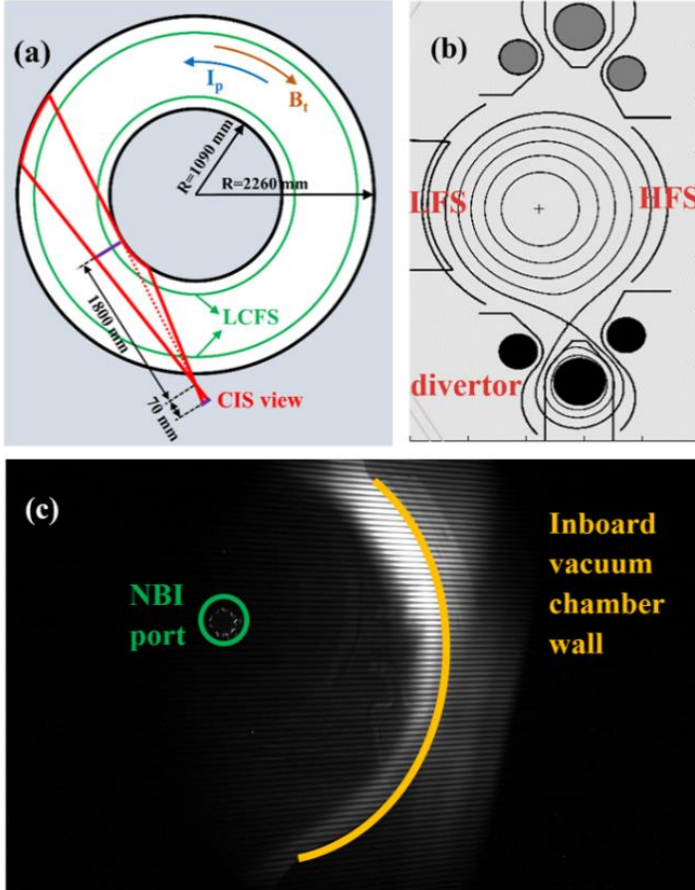


Figure 4. (a) CIS field of view on the HL-2A tokamak; (b) a typical equilibrium configuration reconstruction from EFIT on HL-2A; (c) a CIS raw image of plasma cross section.

A calibration system for HL-2A CIS diagnostic was designed and applied in the laboratory, as shown in Figure 5. The light source is a custom tunable diode laser. It features mode-hop free wavelength tuning around CIII triplet lines for CIS diagnostic. The accuracy of wavelength adjustment is \sim pm. It's feasible to use it to simulate the CIII spectral line with/without doppler shift. A polarizing cube is used to split the laser beam into two beams. Their intensity ratio can be adjusted by rotating the half-wave plate. One beam is coupled to a high precision wavelength meter via a fiber. The stated accuracy of this wavelength meter is \sim 0.1 pm. Another beam illuminates a modular integrating sphere and outputs a uniform circular spot. It generates a calibration interferogram at a certain wavelength via CIS interferometer.

Figure 6(a) shows the wrapped phase demodulated from the interference fringe pattern

of CIII line without doppler shift, i.e. $\phi(\lambda_0)$. Figure 6(b) shows the calibration result for group delay $\hat{N}(\lambda_0)$. The range of wavelengths used in the group delay calibration is [461.6, 466.1] nm. The demodulated phase shift $\Delta\phi$ for each wavelength shift is the average of phase shifts over the central image (50x50 pixels). It is marked with blue rectangular point. $\hat{N}(\lambda_0) = 1394.5 \pm 0.4$ is obtained via a second-order polynomial fit (green dashed line) of these points. The red rhombic points shows the theoretical results based on Sellmeier equations[22]. The theoretical group delay for stated α -BBO waveplate thickness = 4.6mm is 1439.4. It's different from the fitting result from the actual measurements. This demonstrates that the theoretical prediction does not give an accurate group delay due to the imprecise stated thickness. Since the demodulated phase is wrapped into $(-\pi, \pi]$, thus $|\phi_D| < \pi$ to get rid of phase jump. Substituting this into equation (4), the measured largest line-averaged flow velocity $v_{max} = c/2\hat{N}(\lambda_0) \approx 108$ km/s. This is about 5 times larger than plasma flow velocity in the SOL and divertor region of the HL-2A tokamak. So, there won't be phase jump problem for this system.

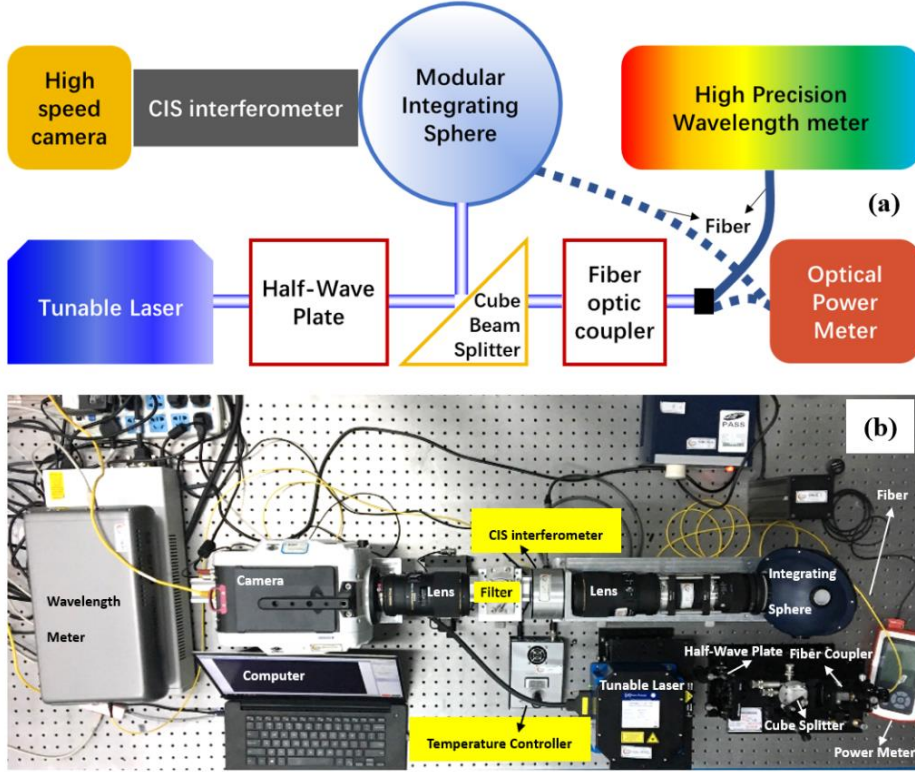


Figure 5. (a) Schematic and (b) photo of CIS calibration system in the laboratory.

The absolute phase of the fringes is very sensitive to changes in the ambient temperature and the alignment of the birefringent crystals [9, 19, 20]. The instrument temperature must be stabilized and the phase must be calibrated regularly at the CIII rest wavelength, to avoid any systematic error in the inferred flow velocity. Unfortunately, it was not possible to install the laser calibration system in the HL-2A experiment hall, so direct calibration for the measurements presented in this work is not available. Thus, an alternative procedure is necessary. Here, we rely on a similar technique to that presented in previous work [20], where the parameters of an instrument model are optimized to

match phase images measured in the lab over a range of wavelengths using the tunable laser. The phase predicted by this optimized model is, to within some fixed offset, significantly less sensitive than the calibration itself and so remains valid after installation of the instrument on HL-2A. The model allows for accurate ($\sim \pm 1$ km/s) extrapolation of phase images measured at a nearby spectral lamp line (Cd I 467.81 nm) to the required stationary CIII wavelength. The lamp measurement was made regularly throughout the day during the HL-2A measurements. This calibration procedure will be fully described in a planned future paper[23].

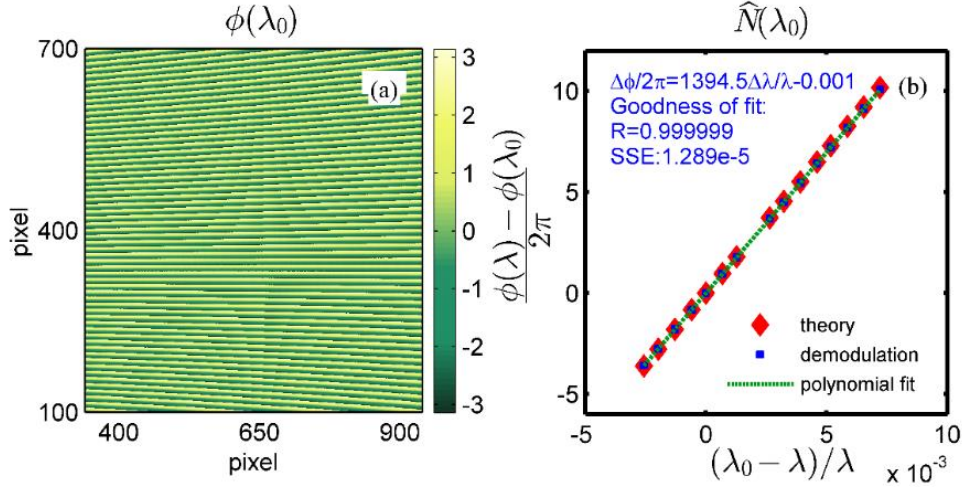


Figure 6. (a) The fringe pattern of CIII line without doppler shift, i.e. $\phi(\lambda_0)$; (b) Calibration for $\hat{N}(\lambda_0)$: the group delay of the birefringent crystal for CIII line.

3. Measurements for carbon impurity flow in H-mode

The Doppler CIS diagnostic was put into operation in the latest campaign (2018-2019) on the HL-2A tokamak. This system took raw images of interferogram of CIII lines emitted from plasma in the scrape off layer of high field side. Two-dimensional brightness images and phase images were extracted from the raw images. Combined with the calibration for group delay and fringe pattern without doppler shift, images of C^{2+} sight-line-averaged flow can be calculated by equation (4). The frame rate ranged from 100 Hz to 2 kHz limited by the light intensity in the campaign.

Figure 7 shows the 2-D measuring results by Doppler CIS in a H mode discharge with divertor configuration on the HL-2A tokamak. The discharge parameters are shown below: $I_p \sim 160$ kA, $B_t \sim 1.27$ T, $n_e \sim 2.0-2.6 \times 10^{19} m^{-3}$. The LHCD heating power is 500 kW and NBI in co- I_p direction heating power is 700 kW. The plasma stored energy is 25-35 kJ. The frame rate of camera is 1 kHz. The resolution is 1280x800 pixels. Figure 7(a1-a5) show the 2-D images of line-integrated emissivity, $I_0 = \int e(r) dl$, where $e(r)$ is local emissivity. The time 1130-1134 ms is corresponding to a period of edge-localized modes (ELM), as marked by the green rectangle in Figure 8. Figure 7(b1-b5) show the evolution of 2-D images of line-averaged flow, $v_D = \int e(r) \vec{v}(r) \cdot d\hat{l} / I_0$, where $\vec{v}(r)$ is the local flow. $v_D > 0$ is corresponding to co- I_p direction, while $v_D < 0$ is corresponding to counter- I_p direction. These results show the carbon plasma flow velocity is ~ 10 km/s. During ELM crash phase, the CIII light intensity increases sharply

and the carbon plasma flow increases in co-Ip direction obviously, especially in the region above the inner mid-plane. A complicated flow pattern is found when looking at the whole cross section.

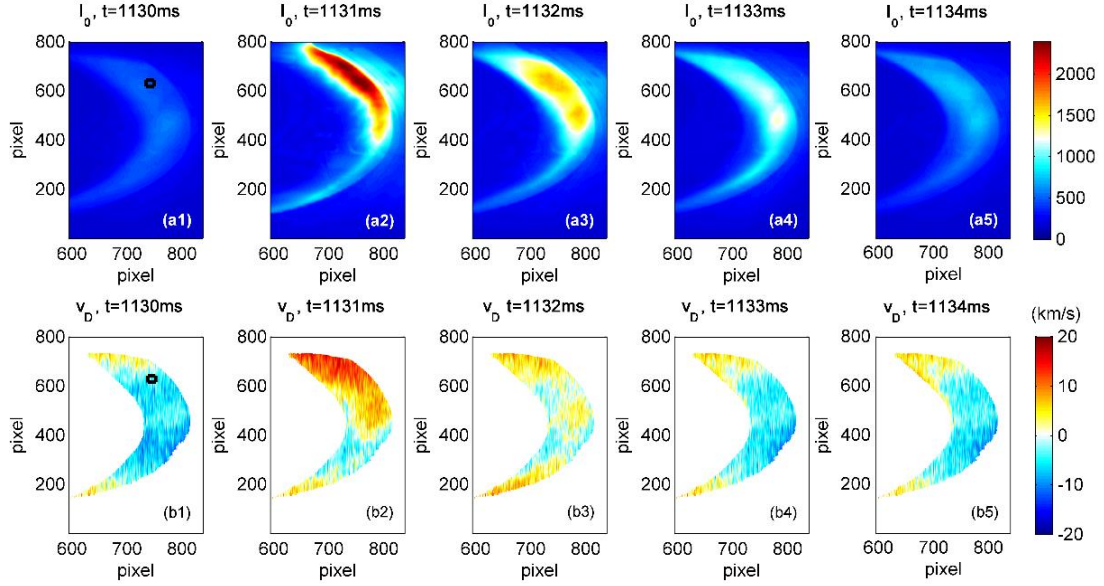


Figure 7. Results for CIII emission and flow measurements by Doppler CIS in an ELMy H-mode discharge on the HL-2A tokamak: (a1-a5) the line-integrated emission images for CIII; (b1-b5) the line-averaged flow images for CIII; in a period of edge-localized modes.

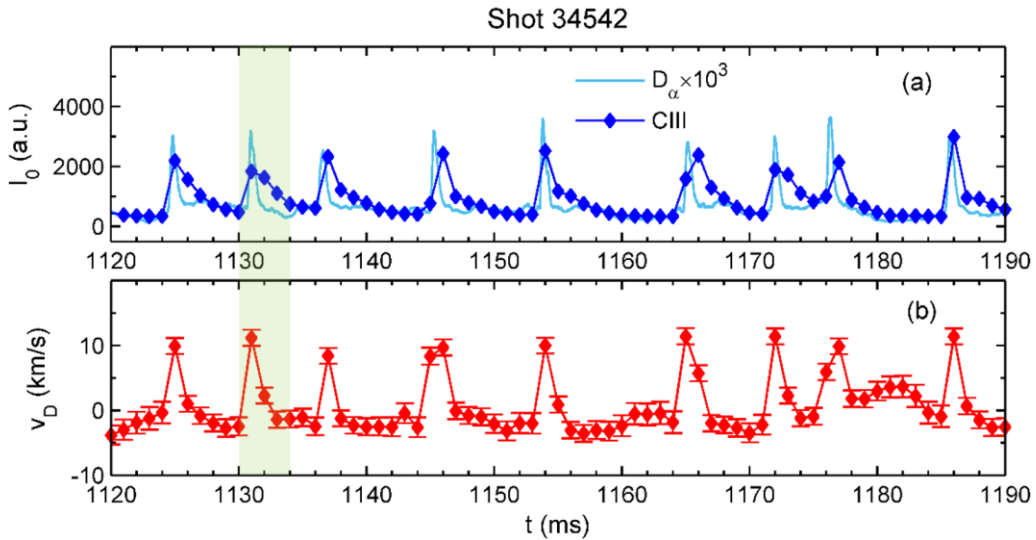


Figure 8. (a) The time trace of CIII light intensity in the area marked by black rectangle in Figure 7(a1) and D_α signal in the divertor; (b) the time trace of C^{2+} flow in the same area marked by black rectangle in Figure 7(b1).

Figure 8(a) shows the time trace of CIII light intensity in the area marked by black rectangle in Figure 7(a1) over the course of many ELM crashes. It exhibits a similar trend with D_α signal in divertor. Figure 8(b) shows the time trace of C^{2+} flow in the

same area. The rapid velocity variation of ~ 10 km/s in co- I_p direction coincides with ELM crashes. The error bar ~ 1 km/s is estimated from the error introduced by image noise, phase demodulation process and group delay calibration fitting. The flow velocity exhibits comparable magnitudes and a similar trend with toroidal velocity measurement from Mach probes in SOL from similar discharges[24]. This suggests that the CIS measurements give plausible results.

4. Summary and future work

A Doppler coherence imaging spectroscopy diagnostic for 2-D imaging of sight-line-averaged impurity flow in the SOL, has been developed on the HL-2A tokamak. A custom optical system and a delicate calibration system have been built and applied for this diagnostic. The spatial angular resolution in horizontal direction is $\sim 0.023^\circ$, and the spatial angular resolution in vertical direction is $\sim 0.25^\circ$, over a 33.6° field of view. Temporal resolution up to 1ms has been achieved in ELMy H-mode discharges on the HL-2A tokamak. Inferred C^{2+} flow on the high field side SOL region shows complicated flow pattern and rapid variation of ~ 10 km/s in co- I_p direction during ELM crash phase. The flow velocity exhibits comparable magnitudes and a similar trend with toroidal velocity measurement from Mach probes in SOL from similar discharges. This suggests that the CIS measurements give plausible results.

Tomographic inversion of the CIS measurement data to obtain local emissivity and flow results is postponed to the future work. Besides, to avoid the need for spectral lamps and complicated phase extrapolation modelling, installing the calibration system in the HL-2A machine hall for regularly automatic phase calibration is also scheduled. In the longer term, coherence imaging spectroscopy diagnostic are planned to apply to the HL-2M[25], which is a new tokamak under construction to explore high-performance tokamak plasma operation regimes.

Acknowledgements

The authors would like to thank Cao Mingyun, Chen Wenjin, He Xiaoxue for their help. The authors would also like to acknowledge discussions with Dr. J. Harrison and Dr. N. Conway. This work is supported by National Key R&D Program of China under 2017YFE0301201, 2018YFE0309103 and 2017YFE0300405, National Natural Science Foundation of China under Grant No. 11705052, 11875124, U1867222, 11575055 and 11905050, and Chinese National Fusion Project for ITER under Grant No. 2015GB120002 and 2015GB104003. The work is also supported by the UK Funder XXX under No. XXX and UK Funder XXX under No. XXX?

References

- [1] Shimada, M., et al., Nuclear Fusion, 2007. **47**(6): p. S1-S17.
- [2] LaBombard, B., et al., Nuclear Fusion, 2004. **44**(10): p. 1047.
- [3] Doyle, E.J., et al., Nuclear Fusion, 2007. **47**(6): p. S18.
- [4] Howard, J., et al., Plasma Physics and Controlled Fusion, 2003. **45**(7): p. 1143-1166.
- [5] Howard, J., Review of Scientific Instruments, 2006. **77**(10): p. 10F111.
- [6] Howard, J., Journal of Physics B: Atomic, Molecular and Optical Physics, 2010. **43**(14): p. 144010.
- [7] Lester, R., et al., Plasma Sources Science and Technology, 2016. **25**(1): p. 015025.
- [8] Chung, J., et al., Plasma Physics and Controlled Fusion, 2005. **47**(6): p. 919-940.
- [9] Gradic, D., et al., Fusion Engineering and Design, 2019. **146**: p. 995-998.
- [10] Howard, J., et al., Review of Scientific Instruments, 2010. **81**(10): p. 10E528.
- [11] Howard, J., et al., Contributions to Plasma Physics, 2011. **51**(2 - 3): p. 194-200.
- [12] Silburn, S.A., et al., Review of Scientific Instruments, 2014. **85**(11): p. 11D703.
- [13] Howard, J., et al., Review of Scientific Instruments, 2016. **87**(11): p. 11E561.
- [14] Xu, M., et al., Nuclear Fusion, 2015. **55**(10): p. 104022.
- [15] Xuru, D., et al., Nuclear Fusion, 2017.
- [16] Ke, R., et al., Review of Scientific Instruments, 2018. **89**(10): p. 10D122.
- [17] Xu, M., et al., Nuclear Fusion, 2019. **59**(11): p. 112017.
- [18] Steel, W.H., *Interferometry*. Vol. 1. 1983: CUP Archive.
- [19] SILBURN, S., *A Doppler coherence imaging diagnostic for the mega-amp spherical tokamak*. 2014, Durham University.
- [20] Samuell, C.M., et al., Journal of Instrumentation, 2017. **12**(08): p. C08016-C08016.
- [21] Allen, S.L., et al., Review of Scientific Instruments, 2018. **89**(10): p. 10E110.
- [22] <http://www.agoptics.com/Alpha-BBO.html>.
- [23] J. S. Allcock et al., to be submitted, 2019.
- [24] Xu, M., et al., *Direct Measurement of ELM Related Momentum Transport in the Edge of HL-2A H-Mode Plasmas*. 2018: 26th IAEA Fusion Energy Conference
- [25] Liu, D.Q., et al., Fusion Engineering and Design, 2013. **88**(6): p. 679-682.